Development 127, 143-153 (2000)
Printed in Great Britain © The Company of Biologists Limited 2000
DEV2417

Targeted disruption of the murine *jun*D gene results in multiple defects in male reproductive function

Dominique Thépot[1,2,*], Jonathan B. Weitzman[2,*], Jacqueline Barra[3], Dominique Segretain[4], Marie-Georges Stinnakre[5], Charles Babinet[3] and Moshe Yaniv[2,§]

[1]Laboratoire de Biologie Cellulaire et Moléculaire, and [5]Laboratoire de Génétique Biochimique, INRA, 78352 Jouy-en-Josas Cedex, France
[2]Unité des Virus Oncogènes CNRS URA 1644, and [3]Unité de Biologie du Développement CNRS URA 1960, Institut Pasteur, 75724 Paris Cedex 15, France
[4]Groupe d'Etude des Communications Cellulaires, Université Paris V, 75006 Paris, France
*The first two authors contributed equally to this work
[§]Author for correspondence (e-mail: yaniv@pasteur.fr)

Accepted 12 October; published on WWW 8 December 1999

SUMMARY

JunD is one of three mammalian Jun proteins that contribute to the AP-1 transcription factor complex. Distinct regulation and functions have been proposed for each Jun member, but less is known about the biological functions of each of these proteins in vivo. To investigate the role of JunD, we have inactivated the murine gene by replacement with a bacterial *lacZ* reporter gene. Embryonic JunD expression was initially detected in the developing heart and cardiovascular system. Subsequent broadening phases of JunD expression were observed during embryonic development and expression in the adult was widespread in many tissues and cell lineages. Mutant animals lack JunD mRNA and protein and showed no evidence of upregulation of c-Jun and JunB mRNA levels. In contrast to the other two Jun members, homozygous JunD$^{-/-}$ mutant animals were viable and appeared healthy. However, homozygous JunD$^{-/-}$ animals showed a reduced postnatal growth. Furthermore, JunD$^{-/-}$ males exhibited multiple age-dependent defects in reproduction, hormone imbalance and impaired spermatogenesis with abnormalities in head and flagellum sperm structures. No defects in fertility were observed in JunD$^{-/-}$ female animals. These results provide evidence for redundant functions for members of the Jun family during development and specific functions for JunD in male reproductive function.

Key words: AP-1, Growth, Infertility, Spermatogenesis, Mouse, *jun*D

INTRODUCTION

JunD is a member of the mammalian Jun family of proto-oncogenes, which includes c-*jun* and *jun*B (Angel et al., 1988; Bohmann et al., 1987; Hirai et al., 1989; Ryder et al., 1989). Each Jun protein can form either homodimers or heterodimers with members of the related Fos family (c-Fos, FosB, Fra-1 and Fra-2) or with the ATF family (ATF2, ATF3 and ATF4) to create the AP-1 transcription factor (Angel and Karin, 1991; Hai et al., 1989). Jun/Jun and Jun/Fos dimers bind to the TPA responsive element (TRE) TGACTCA present in many gene promoters, whereas Jun/ATF dimers bind preferentially to the cAMP responsive element (CRE) TGACGTCA (Angel and Karin, 1991).

The Jun and Fos factors are basic-leucine zipper (bZIP) proteins characterised by a basic DNA-binding domain joined to a C-terminal leucine zipper dimerisation domain (Kouzarides and Ziff, 1988; Landschulz et al., 1988; Sassone-Corsi et al., 1988). The three Jun proteins are similar in their interaction with Fos members and in DNA-binding affinity (Nakabeppu et al., 1988). The N-terminal transactivation domain is less conserved and may account for the different transactivation characteristics of the Jun proteins. For example, the c-Jun protein contains a binding site for the Jun N-terminal Kinase (JNK) and phosphorylation of adjacent serine residues enhances its transactivation potential (Smeal et al., 1991). JunD contains the N-terminal serine residues, but lacks a functional JNK docking site (Kallunki et al., 1996) and is a weaker transcriptional activator. The JunB protein contains a JNK-binding site, but lacks the appropriate residues flanking the phospho-acceptor sites (Chiu et al., 1989). Hence, the three Jun proteins differ in their regulation by JNK and in their transactivation characteristics.

Further differences in the biological functions of the Jun proteins may result from differential expression. High *jun*D mRNA levels were observed in a range of tissues (Hirai et al., 1989; Ryder et al., 1989), whereas the other two *jun* genes have a restricted expression pattern (Wilkinson et al., 1989). Indeed, in situ analysis suggested that the distribution of different *jun* genes are non-overlapping in many organs. Tissue-specific expression of c-Jun and JunB during embryogenesis and organogenesis suggested distinct developmental roles

(Wilkinson et al., 1989). Differences have also been recorded in specific adult tissues. For example, the expression of the Jun proteins is restricted to distinct differentiation stages in the skin (Rutberg et al., 1996) and in testes (Alcivar et al., 1991; Cohen et al., 1993). When these patterns are viewed in parallel with the differential expression patterns of the *fos* genes, a complex picture of potential tissue-specific AP-1 dimers emerges. Discerning the function of specific dimers in different cellular contexts presents a challenge to understanding the complexity of AP-1 function in vivo.

Studies examining AP-1 function in vitro have implied distinct functions for individual AP-1 dimers in different cellular contexts, including cell proliferation, cell death and differentiation (Angel and Karin, 1991). For example, c-Jun has been specifically implicated in the control of cell death (Bossy-Wetzel et al., 1997; Ham et al., 1995) and *ras*-induced transformation (Johnson et al., 1996; Mechta et al., 1997). Opposing roles for c-Jun and JunD have been proposed based on differences in cell cycle regulation, mitogenic stimulation and oncogenic transformation. (Kovary and Bravo, 1991; Lallemand et al., 1997; Pfarr et al., 1994). Furthermore, JunD was shown to interact with menin, the product of the *MEN1* tumor suppressor gene, supporting a role for JunD in growth inhibition (Agarwal et al., 1999). Hence, differential regulation of the Jun proteins may coordinate distinct responses to extracellular stimuli.

Several groups have used gene targeting to investigate the functions of individual AP-1 components in vivo. Disruption of the c-*jun* or *jun*B genes resulted in embryonic lethality, indicating essential, nonoverlapping roles during mammalian development. Mice lacking c-Jun die at E12.5 and have a defect in hepatogenesis, whereas mice lacking JunB die earlier with defects in the extraembryonic tissues (Hilberg et al., 1993; Johnson et al., 1993; Schorpp-Kistner et al., 1999). Furthermore, disruption of the c-*fos*, *Fos*B or *ATF2* genes also resulted in distinct phenotypes. Interestingly, these three mutations produced viable mice with varied defects in bone development, growth, spermatogenesis and animal behaviour (Brown et al., 1996; Grigoriadis et al., 1994; Gruda et al., 1996; Johnson et al., 1992; Reimold et al., 1996; Wang et al., 1992). However, we still understand relatively little about the functions played by individual Jun proteins and distinct AP-1 dimers in developing and adult organisms.

Here we report the generation of a null allele for the murine *jun*D gene by replacement with a *lacZ* cassette. These animals enabled us to characterise the expression pattern of *jun*D during development and the phenotype of mice lacking JunD (JunD$^{-/-}$ mice). In contrast to the other two murine *jun* genes, mutation of the *jun*D locus produced homozygous JunD$^{-/-}$ mice which are viable. Homozygous mice exhibited a postnatal growth retardation. Furthermore, male JunD$^{-/-}$ mice exhibit significantly reduced fertility, characterised by defects in mating behaviour and a specific block in spermiogenesis. These results emphasise the complexity of unravelling specific physiological functions for individual AP-1 dimers.

MATERIAL AND METHODS

Construction of JunD targeting vector

A library of mouse 129/Sv genomic DNA was screened with a JunD cDNA probe (Hirai et al., 1989). One phage was isolated that included the 5′ flanking sequence, the entire coding region and 1.9 kb of 3′ sequence. Two different genomic fragments, an *Eco*RI-*Not*I fragment of 6.2 kb from the 5′ flanking region and a *Sph*I-*Eco*RI fragment of 2.4 kb from the 3′ region, were used to construct a replacement vector in which the complete *jun*D coding region was replaced by a NLS-*lacZ* reporter gene and a PGK-neoR cassette. Briefly, a *jun*D promoter fragment (–140 to +120) was amplified by PCR and cloned into the pucBM20 vector (Boehringer). A *Bam*HI-*Hin*dIII NLS-*lacZ* cassette was inserted at the *Hin*dIII site downstream of the promoter. A *Not*I-*Sal*I fragment encompassing the 260 bp of the promoter followed by the *lacZ* gene was excised and clone upstream of the PGK-neoR cassette of a modified pPNT plasmid containing the 2.4 genomic fragment from the 3′ region. The 6.2 kb 5′ genomic fragment was cloned into a Bluescript plasmid (Stratagene) and a 5.6 kb *Sal*I-*Not*I fragment was subcloned into the pPNT modified plasmid to give the targeting vector (Fig. 1A). Finally, the PGK-Thymidine Kinase cassette was inserted at the 3′ end of the vector to generate the final construct.

ES cell culture and generation of chimeric mice

ES cells from the CK35 line were provided by C. Kress (Kress et al., 1998) and were maintained as previously described (Camus et al., 1996). For electroporation of the ES cells, 20 μg of the targeting vector linearized using *Sal*I was added to 1.6×10^7 CK35 cells in phosphate buffer saline (PBS). Electroporation and selection of G418 and Ganciclovir-resistant colonies were performed as previously described by Colucci-Guyon and colleagues (Colucci-Guyon et al., 1994). Chimeric mice were generated from recombinant ES cells as described (Bradley, 1987).

Nucleic acid and protein analysis

Southern blot analysis of genomic DNA, extracted from ES cell clones or mouse tails, was performed following *Eco*RV digestion, blotting onto Hybond-N membranes (Amersham) and probed with an *Eco*RV-*Eco*RI DNA fragment located upstream of the homologous region (Fig. 1A,B).

Genotype analysis was performed by PCR amplification of genomic DNA using four oligonucleotide primers, two mapping within the *junD* gene: 5′-TCGCTCTTGGCAACAGCGGCCGCCACCAGG-3′; 5′-GGCCGCTCAGCGCCTCCTCGCCATAGAAGG-3′ and two in the *lacZ* gene: 5′-GCATCGAGCTGGGTAATAAGCGTTGGCAAT-3′, 5′-GACACCAGACCAACTGGTAATGGTAGCGAC-3′. The size of the amplified bands corresponding to the wild-type or mutant alleles were 315 bp or 812 bp, respectively (Fig. 1C).

Northern blot analysis was performed by standard methods using total RNA extracted from adult mice tissues. RNA (20 μg/lane) were separated in 1.5% agarose gels, transferred to Hybond-N membranes (Amersham) and probed with cDNA fragments radiolabelled by random priming. The JunD probe was a 900 bp *Sph*I fragment of the cDNA (Hirai et al., 1989). The JunB probe was a 1.4 kb *Eco*RI fragment covering the entire coding region of the gene. For c-Jun the probe was a 950 bp *Acc*I fragment covering the 3′ part of the cDNA (Ryseck et al., 1988). The membranes were also probed with a β-actin probe as a control for equal gel loading. Analysis was performed using a PhosphoImager apparatus (Molecular Dynamics).

Jun protein levels were analysed by western blotting. Embryonic fibroblasts were isolated from E13-E14 embryos and whole cell extracts prepared from early passage cells. Extracts (20 μg/lane) were separated by electrophoresis in 10% polyacrylamide gels, electroblotted onto nitrocellulose (BioRad) and the membranes were incubated with antibodies for specific Jun proteins as previously described (Lallemand et al., 1997; Pfarr et al., 1994).

Analysis of gene expression by RT-PCR

Total RNA was isolated from the testes of sterile JunD$^{-/-}$ mice and fertile wild-type controls. cDNA was prepared from 2 μg RNA using random hexaprimer oligonucleotides as templates, in a 25 μl reaction volume containing 1 μl SuperScript II (GIBCO/BRL) reverse

transcriptase (RT) enzyme following the manufacturers' instructions. Samples were diluted to 100 µl before PCR amplification. Samples omitting RT enzyme were used as negative (–RT) controls. Amplification was carried out in 25 µl reactions containing 1 µl cDNA and 1 µM oligonucleotide primers and 0.25 µl TAQ polymerase (Promega). PCR was performed in a Perkin Elmer thermocycler and consisted of 30 cycles of 94°C for 1 minute, 54°C for 1 minute, and 72°C for 1 minute. PCR products (10 µl aliquots) were analysed by agarose gel electrophoresis. The primers used for PCR were: β-actin (5′-GACCTGACAGACTACCTCAT and 5′-AGACAGCACTGTGTTGGCAT), HPRT (5′-CTGGTGAAAAGGACCTCTCG and 5′-CACAGGACTAGAACACCTGC), Hox1.4 (Nantel et al., 1996), protamine 1 (Nantel et al., 1996), protamine 2 (Nantel et al., 1996), transition protein 1 (Nantel et al., 1996), calspermin (Nantel et al., 1996), RT7 (5′-GTTGTCTATGATGTATGAGGCC and 5′-TAGTGTTCCTGGTTACCATGCC) and BMP8 (5′-AAGTCCGAGATGGCTATGCG and 5′-CATGAAAGGCTGTCTGGAGC).

Staining and histological analysis

For X-gal staining, embryos or adult tissues were dissected, fixed in 4% paraformaldehyde/PBS for 20 minutes, washed three times in PBS, and then incubated at 32°C for 3 hours to overnight in a staining solution containing 2 mM $MgCl_2$, 4 mM $K_3Fe(CN)_6$, 4 mM $K_4Fe(CN)_6$, 0.4 mg/ml 4-chloro-5-bromo-3-indolyl-b-D-galactopyranoside (X-gal) and 0.1% Triton in PBS.

For histological analysis, freshly dissected testes were fixed in Bouin's fixative for 24 hours. They were then rinsed and embedded in paraffin. Sections (7 µm thick) were mounted, dewaxed and stained with Eosin/Hematoxylin before examination.

For X-gal staining of histological sections, either the tissues were fixed and stained prior to embedding in paraffin and sectioning (testes and brain), or animals were perfused, tissues removed, embedded in paraffin and sectioned (7 µm thick) prior to X-gal staining. Sections were counterstained with Eosin.

For the analysis of various parameters of epididymal sperm in adult mice, animals were killed and sperm removed from the epididymis, followed by measurements of sperm concentration, motility and morphology as previously described (Albert and Roussel, 1984). For the quantification of germ cell populations in the seminiferous tubules, a mini-programme was developed (courtesy of B. Deleau) using Visilog 4.15 (NOESIS, Les Ulis, France). Briefly, the program was developed to count the number of cells of each distinct lineage. The values represent the number of cells per field (×40 magnification), which corresponds to approximately half of a seminiferous tubule.

Electron microscopy

Homozygous mutant and wild-type mice were anaesthetised with ether and perfused intracardially with a solution of 3.5% glutaraldehyde in either 0.1 M cacodylate buffer (pH 7.4) or 0.1 M PBS buffer (pH 7.4). Testes were removed and immersed in the same fixative for 1 hour, and then minced into small blocks (1 mm^3) and postfixed for an additional hour at room temperature. Samples were then rinsed overnight at 4°C either in PBS or cacodylate buffer, postfixed for 1 hour at 22°C with ferrocyanide-reduced osmium tetroxide (Karnovsky, 1971), dehydrated with graded alcohols and embedded in Epon. Thin electron microscopy sections were counterstained with lead citrate and examined with a Philips CM 10 electron microscope at 60 kV (Institute A. Feyssard, CNRS, Gif-sur-Yvette, France).

Hormone analysis

Quantification of hormones was performed using commercially available kits following the manufacturer's instructions; testosterone Coatria assay kit (BioMérieux, France); rat LH, rat FSH and rat GH using BIOTRAK radioimmunoassay kits (Amersham, UK); inhibin B dimer assay kit (Serotec, UK).

RESULTS

Targeted mutagenesis of the mouse *jun*D gene

The *jun*D gene was disrupted by homologous recombination in CK35 ES cells using a replacement targeting strategy (Fig. 1A). As the murine *jun*D gene contains no introns, a region covering the entire coding sequence was replaced with a *NLS-lacZ*/PGK-neo^R cassette (Fig. 1A). The modified bacterial β-galactosidase

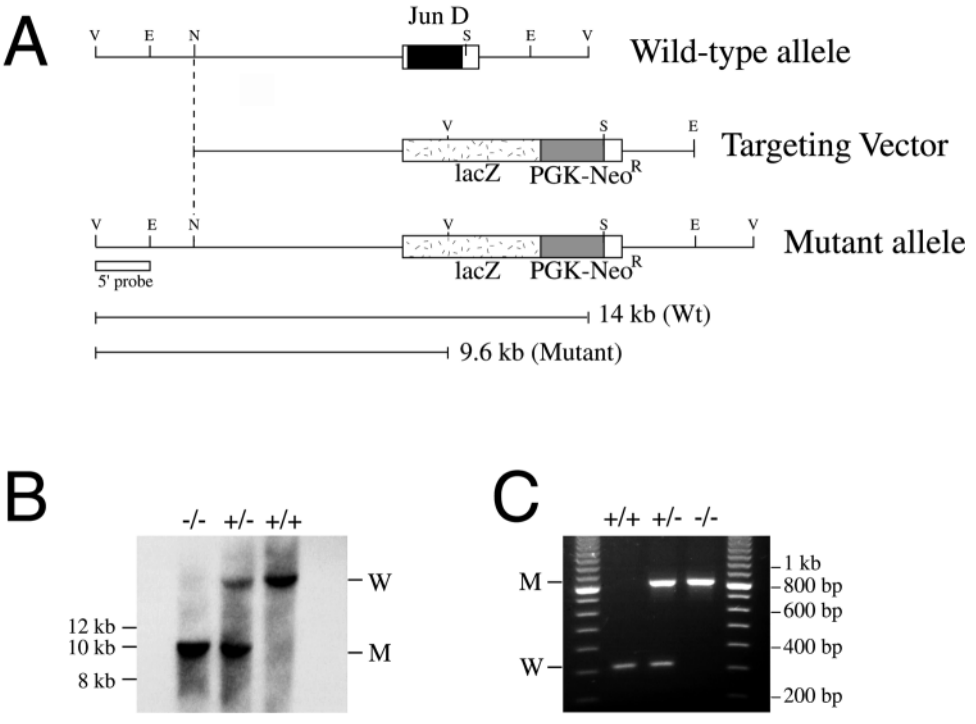

Fig. 1. Targeted mutagenesis of the murine JunD locus. (A) Schematic representation of the wild-type *jun*D allele, the targeting vector, and recombined mutant *jun*D-*lacZ* allele. The transcribed sequences of the *jun*D gene are represented by black (coding sequence) and white boxes (5′ and 3′ UTR). The NLS-*lacZ* cassette and the PGK-NEO^R selection cassette are also indicated. The position of the 5′ probe used for Southern blot analysis is shown, as well as the *Eco*RV-digested fragments of 14 kb (wild type) and 9.6 kb (mutant allele). Restriction endonuclease sites are indicated; C, *Nco*I; E, *Eco*RI; *N*, *Nde*I; O, *Not*I; S, *Sph*I; V, *Eco*RV. (B) Southern blot analysis of *Eco*RV-digested DNA from wild-type (+/+), heterozygous (+/–) or homozygous (–/–) mice. Hybridisation using the 5′ probe yielded bands corresponding to fragments of 14 kb for the wild-type allele (W) or 9.6 kb for the targeted allele (M). (C) PCR genotyping of progeny. Wild-type (+/+), heterozygous (+/–) and homozygous (–/–) mice were identified by the amplification of PCR products specific for either the *jun*D wild-type allele (W, 315 bp) or the targeted allele (M, 812 bp).

gene (*NLS-lacZ*) was placed under the control of the endogenous *jun*D promoter. The PGK-neo^{R} and PGK-TK cassettes were used for positive and negative selection (Mansour et al., 1993). Following electroporation and drug selection, 320 ES clones were selected and analysed. Homologous recombinants were detected by Southern blot analysis of *Eco*RV-restricted genomic DNA using an upstream probe (Fig. 1A). The wild-type allele produced a 14 kb fragment and the targeted allele a 9.6 kb fragment (Fig. 1B). Analysis resulted in the identification of 16 clones in which a recombination event had occurred at the locus. A clone showing the presence of the appropriate 9.6 kb fragment when probed with either the upstream or *lacZ* probes was injected into C57BL/6 blastocysts and four male chimaeras were obtained. Three of these were crossed with female mice to generate heterozygous (JunD$^{+/-}$) mice in both mixed C57BL/6×129/Sv and pure 129/Sv genetic backgrounds. Heterozygous animals were indistinguishable from wild-type littermates.

Expression of *jun*D-*lacZ* in embryos and adult mice

We used heterozygous JunD$^{+/-}$ mice to document the expression of the *NLS-lacZ* transgene under the control of the endogenous *jun*D promoter during embryonic development. No X-gal staining was detected in blastocysts prior to implantation. The earliest *lacZ* expression was detected in the ectoplacental cone at 7.5 days postcoitus (E7.5; Fig. 2A). At day E8.5, β-galactosidase activity was detectable only in small groups of cells in the yolk sac (not shown). Embryonic X-gal staining was observed as early as day E9.5 in the large blood vessels and the developing cardiovascular system (Fig. 2B). As embryogenesis progressed, there was a broadening of the *lacZ* expression pattern in phases. By day E10.5, extensive X-gal staining was observed along the central nervous system, the neural tube and somites, and in the developing musculature (Fig. 2C). There was additional expression in the developing limb bud, in the otic vesicle and the eye. By later embryonic stages (e.g. staining at E15.5, Fig. 2D), the expression was more widespread and roughly mirrored that seen in the adult animal. Hence, this cumulative expansion in phases resulted in a broad staining pattern at the end of development. At these later stages, nearly all the major organs were stained. However, the expression was not uniform; within each organ, *lacZ* expression was observed in particular cell types. Also, some cell types, notably the parenchymal cells of the liver, were almost devoid of staining.

Analysis of X-gal staining in heterozygous JunD$^{+/-}$ adults revealed a similarly wide pattern of expression. However, variations were observed in the intensity of staining. Particularly striking patterns were observed in the heart, kidney and brain (Fig. 3). The strong cardiac staining noted in early embryos persisted in adults (Fig. 3A). Examination of tissue sections indicated that many cells in the heart show a strong nuclear *lacZ* expression, including both cardiac and smooth muscle cells (Fig. 3B). In the adult kidney, X-gal staining was observed both in the medulla, where the blood vessels and the collecting ducts were stained, and in the cortex where the staining of the glomerular structures was clearly visible in histological sections (Fig. 3C,D). Analysis of X-gal staining in the brains of heterozygous animals revealed a striking pattern of expression in neuronal and glial cell populations, with particularly strong staining in the cerebellum, in the cortex and the hippocampus (Fig. 3G,H). *lacZ* expression was also detected in the testis (Fig. 3E), with staining

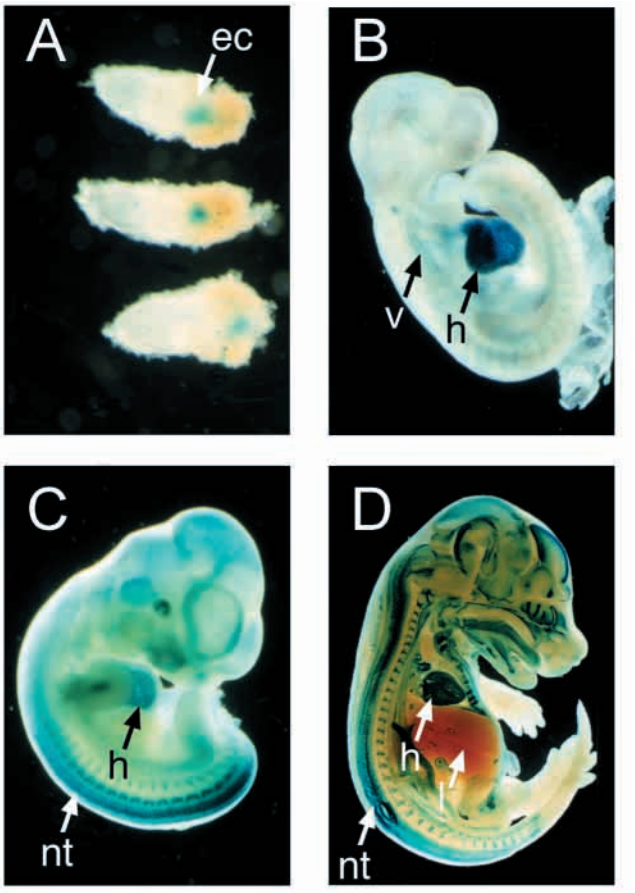

Fig. 2. Expression of the *jun*D-*lac*Z allele during embryonic development. Heterozygous JunD$^{+/-}$ mutant embryos were isolated at different stages during development and the expression of the NLS-*lacZ* protein was detected by in toto staining with X-gal substrate. (A) Three embryos at E7.5 showing staining exclusively in the ectoplacental cone. (B) Staining of an E9.5 heterozygous embryo was restricted to the heart and vessels of the developing cardiovascular system. (C) At day E10.5 β-galactosidase activity was detected in a broader expression pattern including the developing central nervous system and musculature. (D) Staining of a longitudinal section of an embryo at day E15.5. The widespread expression pattern is very similar to that seen postnatally. Ec, ectoplacental cone; h, heart; nt, neural tube; v, vessels; l, liver.

of testicular interstitial cells, Sertoli cells and all germ cell populations, with the exception of spermatogonia (Fig. 3F). Staining was also observed in the epididymis, which was markedly above the low levels of background staining. Some tissues had notably lower expression levels; for example, in the liver, there was little staining except for the blood vessels or ducts (data not shown). The wide tissue distribution confirmed and extends previous results from northern blot and in situ analysis (Hirai et al., 1989; Ryder et al., 1989).

Phenotypic analysis of homozygous JunD$^{-/-}$ mutant mice

To test whether the broad expression pattern of JunD reflects diverse functions during development, we crossed heterozygous JunD$^{+/-}$ mice and analysed their offspring by Southern blot or PCR screening (Fig. 1B,C). These crosses

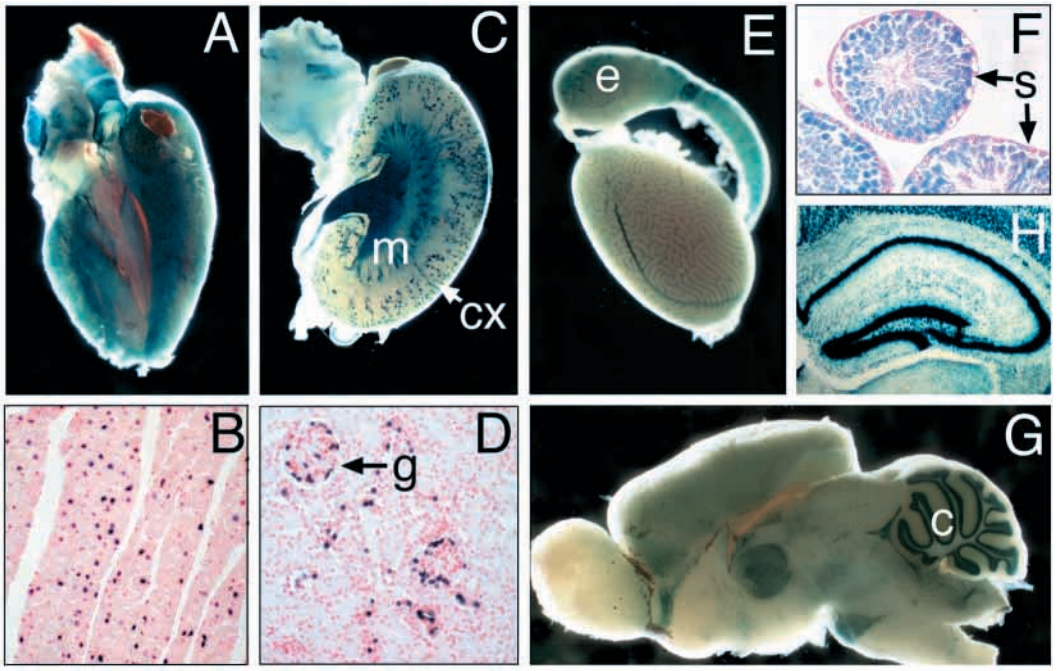

Fig. 3. Expression of the *jun*D-*lacZ* allele in adult tissues. The staining pattern of *lacZ* expression in adult heterozygous mutant mice is shown for the heart (A,B), kidney (C,D), testes (E,F) and brain (G,H). X-gal staining was either performed on whole tissues (A,C,E,G) or on histological sections (B,D,F,H) (×40 magnification). g, glomeruli; cx, cortex; m, medulla; c, cerebellum; e, epididymis; s, spermatogonia.

yielded viable homozygous JunD$^{-/-}$ mice at the predicted ratio of wild-type (*n*=47), heterozygous (*n*=86) and homozygous (*n*=43) mutant offspring. Hence, despite the cumulative, phased expression of JunD during embryogenesis, JunD function is not essential for mouse development.

The homozygous JunD$^{-/-}$ mutant mice appeared similar to wild-type or heterozygous littermates. However, in most litters, the smallest animals were those with the homozygous *jun*D$^{-/-}$ genotype. Mutant and wild-type littermates were weighed and their growth rates compared (Fig. 4). At birth, the average weight of homozygous mice was indistinguishable from littermates (1.78±0.05 g compared to wild-type 1.77±0.02 g). However, with age the weights of the animals diverged and adult body weight represented 80-85% that of wild-type littermates (Fig. 4). At two months of age, the average weight of homozygous males (20.5±2.6 g; *n*=8) was significantly reduced compared to wild-type (25.2±2.5 g; *n*=13) or heterozygous male animals (24.3±2.0 g; *n*=27). Similar results were found with female animals for homozygous (17.6±1.3 g; *n*=13), heterozygous (19.9±1.6 g; *n*=22) and wild-type genotypes (21.1±1.1 g; *n*=12). We carried out extensive histological analysis of the major organs of mutant animals and monitored their behaviour and health for over 18 months. We observed no gross histological abnormalities in the tissues examined (including kidney, brain, stomach, gut, heart, skin, pituitary). Analysis of the immune system revealed no major changes in hematopoetic lineages or severe infection. To investigate the cause of the growth retardation, we quantified growth hormone (GH) levels in the serum of mutant and wild-type adult animals and observed that GH levels were reduced in JunD$^{-/-}$ animals (9.7±1.7 ng/ml, *n*=7) compared to heterozygous (12.7±4.9 ng/ml, *n*=3) or wild-type controls (13.9±3.3 ng/ml, *n*=3). Furthermore, analysis of GH levels in younger (4 week old) litters also revealed a similar 30% reduction in both circulating GH in serum (6.2±1.7 ng/ml in Jun$^{-/-}$ animals, compared to 8.4±1.8 ng/ml in JunD$^{+/-}$ animals) and in total pituitary GH levels (8.3±1.4 μg in Jun$^{-/-}$ animals, compared to 11.5±1.8 μg in JunD$^{+/-}$ animals). These results suggest that reduced growth hormone levels may contribute to the postnatal growth defect of the JunD$^{-/-}$ mutant mice.

The surprisingly mild mutant phenotype could be due to a compensatory upregulation of the other *jun* genes in JunD$^{-/-}$ animals. We investigated this hypothesis by northern blot analysis of *jun* gene mRNA levels. As expected, there was no detectable *jun*D mRNA in the brain, kidneys, lungs, heart, stomach, testis and skeletal muscle of homozygous JunD$^{-/-}$ mice (Fig. 5A and data not shown), confirming that our mutagenesis created a null allele. Also, fibroblasts derived from JunD$^{-/-}$ embryos showed a complete absence of JunD protein by immunoblot analysis (Fig. 5B). The faint band seen in $^{-/-}$ lanes was due to mild cross-reactivity of the anti-JunD antibodies with the c-Jun protein (D. Lallemand, personal communication). Furthermore, we observed no changes in the levels of c-*jun* or *jun*B mRNA levels in the tissues of homozygous JunD$^{-/-}$ mice (including stomach, lungs, brains, kidneys, heart or testis, Fig. 5A and data not shown), compared to control animals. Likewise, there were no changes in the protein levels of c-Jun or JunB in fibroblasts isolated from JunD$^{-/-}$ embryos (Fig. 5B). These results confirm that we have created a null allele for *jun*D and that this does not cause a dramatic compensatory upregulation of the other *jun* genes.

Reproductive defects in homozygous JunD$^{-/-}$ male mice

During attempts to establish a breeding colony, we noticed reduced offspring rates in cages of JunD$^{-/-}$ mice. Therefore, we systematically tested the reproductive capacity of homozygous mice of both sexes with wild-type mates. Homozygous JunD$^{-/-}$ female mice showed no severe reproductive defects and produced litters of approximately normal size (average litter size = 5.6, *n*=27 compared to 6.0, *n*=23 for wild-type females). In contrast, when JunD$^{-/-}$ male

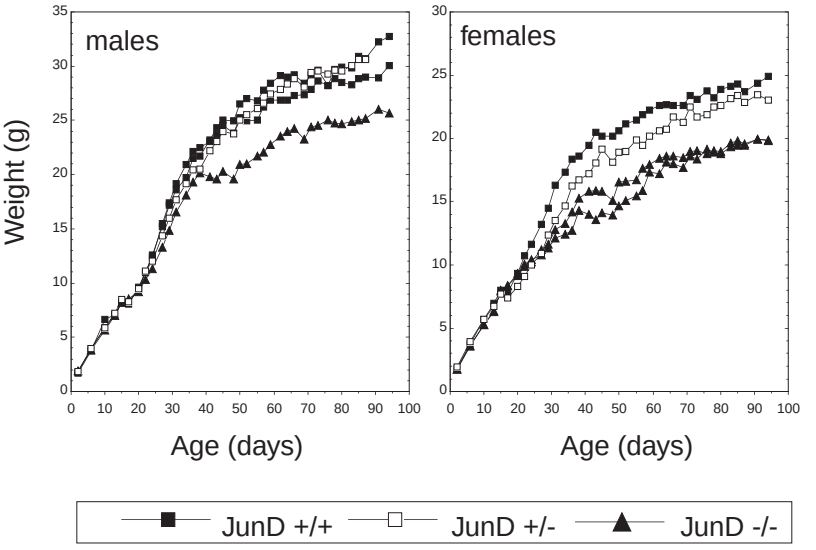

Fig. 4. Reduced growth of homozygous JunD$^{-/-}$ mutant animals. Growth curves of a typical litter from crosses between heterozygous JunD$^{+/-}$ animals. Each individual mouse from a litter containing 4 males (left) and 4 females (right) was weighed every 2-3 days for the first three months of age. Homozygous JunD$^{-/-}$ mice (triangles) of both sexes showed reduced growth compared to heterozygous (open squares) or wild-type (filled squares) littermates.

mice were mated with wild-type females approximately 25% failed to produce any litters over a 2-month breeding period. Furthermore, in the remaining mice, there was a drop in fertility with age; more than half the mice mated normally when young (average litter size = 5.9, *n*=21), but ceased to produce litters as they grew older (Fig. 6A). No such behaviour was observed in heterozygous mice. Similar observations were found in colonies of a pure (129/Sv) or mixed (129/Sv×C57/B6) genetic backgrounds. We focused subsequent experiments on the group of animals that failed to give any litters.

We studied the frequency of copulations of these males over a 2-week period. Observation of the behaviour of these animals in the presence of wild-type females in oestrus, or superovulated females, revealed that they failed to exhibit any mating behaviour or vaginal plugs, whereas control male littermates engaged immediately in mounting behaviour. We examined whether this was due to a deficit in testosterone. Although very variable, testosterone levels did not differ significantly between sterile homozygous males and fertile homozygous, or wild type-males (wild-type = 1.5±1.2 ng/ml, *n*=5; fertile JunD$^{-/-}$ = 2.8±0.9 ng/ml *n*=17, sterile JunD$^{-/-}$ = 2.2±1.2 ng/ml, *n*=9). Moreover, the weight of the seminal vesicle, a testosterone-sensitive organ, in homozygous sterile males (175.6±69.1 mg, *n*=4) was not statistically different from fertile homozygous males (172.3±23.7 mg, *n*=4), or wild-type males (186.8±12.0 mg, *n*=3).

Spermatogenesis defects in homozygous JunD$^{-/-}$ mutant mice

We performed a detailed histological examination of the testes of these sterile animals to search for structural abnormalities of the reproductive tract. A subset of homozygous mice that failed to mate displayed an abnormal testicular histology. Of the 13 sterile animals examined, 5 showed clear testis defects, while the others appeared to be histologically normal. A comparison of several spermatogenic parameters is shown in Table 1. No significant differences were observed in testes weights. The epididymal sperm analysis revealed that the sterility phenotype was heterogeneous and that homozygous mutant mice fall in two classes; group I exhibited oligo-astheno-teratospermia in which most spermatozoa showed frequent head and flagellum abnormalities, whereas group II had sperm of normal concentration and morphology, but with a dramatically diminished sperm motility (asthenospermia) (Table 1).

Light microscopy analysis of the seminiferous tubules of group I sterile mice revealed a striking absence of flagella in the lumen of the tubules (Fig. 6D,E). Detailed quantification of the different cell types in mutant mice tubules revealed that the numbers of Sertoli cells, spermatogonia, early spermatocytes and round spermatids were not affected at any stage of spermatogenesis (Fig. 6F,G). However, in stage VII tubules, the total absence of the flagella in the mutant animals correlated with a marked decrease in the number of late spermatid heads located near the lumen (Fig. 6F).

Further characterisation using light microscopy and electron microscopy revealed abnormalities in head and flagellum structures during spermatogenesis. For example, in stage V tubules, the clustering heads of late spermatids inserted inside the seminiferous epithelium showed an abnormal hammer-like shape (Fig. 7A). This flattening of the head was the most frequent malformation observed and was also seen at the ultrastructural level (Fig. 7B). However, the condensation of the nucleus appeared normal. Spermatogenesis appeared to

Table 1. Spermocytogram of homozygous JunD$^{-/-}$ mutants and wild-type mice

	Wild-type JunD$^{+/+}$ males *n*=2	Homozygous JunD$^{-/-}$ males	
		Group I *n*=3	Group II *n*=2
Weight of animal (g)	30.5±0.5	23.8±5.8	24.5±0.5
Weight of testes (mg)	72±4	61±9	98±4
Total sperm number (average)	5.15×10^6	0.54×10^6	5.37×10^6
Sperm motility (%)	5±5.0	0	7.5±2.5
Head abnormalities (%)	5.5±1.5	86.7±3.8	10±1.0
Flagella abnormalities (%)	19.5±3.5	96.0±5.7	18.5±1.5

progress normally until stage III, when the growing flagellum begins to extend from the round spermatids. When the spermatids begin to elongate, malformations of the flagellum were obvious with some disorganisation of microtubules. At later stages, there was a significant decrease in the number of growing flagella and, when the classical microtubule organisation was recognised, it appeared devoid of structures such as radial spokes and dynein arms (Fig. 7D). At the final phase of spermiogenesis, late spermatids present in the tubules showed more flagella defects. When the flagellum merged out of the cell cytoplasm to form the future proximal region of the tail, the periaxonemal cytoplasm bulged out, forming irregular cytoplasmic masses (compare Fig. 7E and F). This irregularly shaped periaxonemal cytoplasm still contained clusters of electron-dense material, as well as disorganised small microtubules.

To attempt to understand this testis phenotype further, we analysed the levels of circulating hormones that regulate the spermatogenic process. Quantification of serum levels indicated a significant increase in inhibin B levels in sterile homozygote JunD$^{-/-}$ animals (13.3±1.5 pg/ml, *n*=10) compared to JunD$^{+/-}$ (10.2±1.1 pg/ml, *n*=15) or wild-type animals (8.3±1.6 pg/ml, *n*=13). There was a corresponding decrease in the levels of follicle-stimulating hormone (FSH) in JunD$^{-/-}$ males (25.4±3.3 ng/ml, *n*=12), compared to JunD$^{+/-}$ (34.7±3.6 ng/ml, *n*=5) or wild-type animals (36.4±3.8 ng/ml, *n*=4). No differences were observed in lutenizing hormone levels. These results suggest that hormone imbalance may contribute to the reduced fertility of JunD$^{-/-}$ males.

To investigate the nature of the spermatogenesis block at the molecular level, we analysed the expression of several genes as spermatogenesis markers. We observed a marked decrease in mRNA levels for *calspermin*, *RT7* and *BMP8* (Fig. 8). In contrast, there were no dramatic changes in the levels of expression of protamine genes, *Hox1.4* or *transition protein 1*. The *calspermin* and *RT7* genes serve as specific markers of the late stages of spermatogenesis. *BMP8* has been associated with the maintenance of adult spermatogenesis (Zhao et al., 1996, 1998). Therefore, the sterility phenotype of JunD$^{-/-}$ males is associated with reduced expression of a subset of spermatogenesis-related genes.

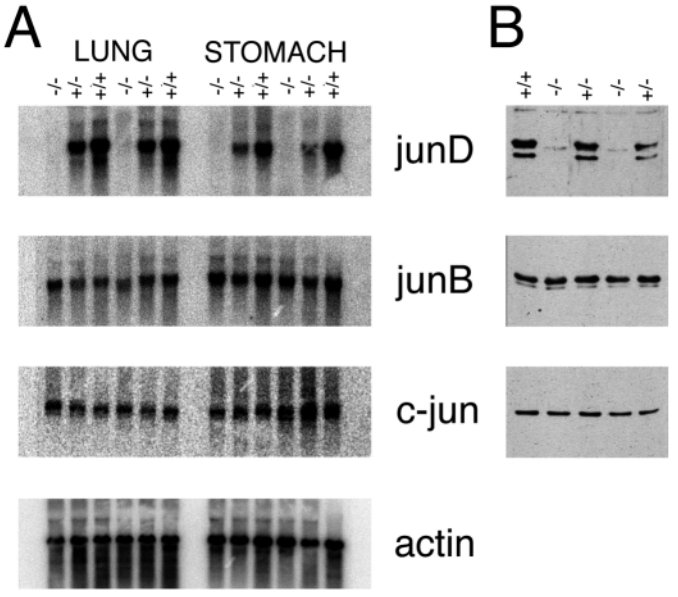

Fig. 5. Analysis of the expression of the *Jun* genes in mutant mice. (A) Northern blot analysis of expression of the three *jun* genes in JunD mutant mice. For each genotype, 20 mg of total RNA were analysed from adult lungs or stomach. Two animals of each genotype were analysed (homozygote $^{-/-}$, heterozygote $^{+/-}$ or wild-type $^{+/+}$). Hybridisation with a β-actin probe was used as a control for equal loading. (B) Western blot analysis of Jun proteins levels. Whole-cell extracts were prepared from embryonic fibroblasts and analysed by immunoblotting using antibodies specific for each Jun family member. Two independently isolated heterozygote (+/–) and homozygote (+/+) fibroblasts were analysed.

DISCUSSION

JunD differs from the other two mammalian Jun proteins in terms of its expression pattern, regulation by mitogens and stress, and its transactivation capacity (Hirai et al., 1989; Kallunki et al., 1996; Pfarr et al., 1994; Ryder et al., 1989). We have generated a null allele for the *jun*D gene by replacing the coding region with a modified *NLS-lacZ* gene, enabling us to document the JunD expression pattern and the phenotype of *jun*D$^{-/-}$ animals. Our results are in marked contrast with studies mutating the genes for c-*jun* or *jun*B. JunD is dispensable for embryonic development, but critical for the maintenance of normal male reproductive functions. These results offer insights into redundant and tissue-specific functions of the individual Jun members.

Expression of JunD during embryonic development and in adult tissues

Analysis of heterozygous *jun*D-*lacZ* embryos revealed the appearance of broadening, cumulative waves of expression during development. These phases were additive in that, once expression was observed, it persisted until adulthood. Each successive phase appeared to follow the initial stages of organogenesis, suggesting a role in the maintenance of specific cell lineages once the commitment to differentiation is established. JunD expression is highest in differentiated cells such as myoblasts, epithelium and postmitotic neurons. This is consistent with earlier studies suggesting that JunD functions in growth inhibition (Pfarr et al., 1994). A role for JunD in the maintenance of specific organ functions is also suggested by the age-related sterility phenotype observed in adult males. As the other two Jun proteins also exhibit specific expression patterns during organogenesis (Wilkinson et al., 1989), we can begin to appreciate how development may be associated with shifts in the ratios of different Jun-containing AP-1 dimers.

The expression analysis in adult animals confirms and extends earlier Northern blotting results (Hirai et al., 1989; Ryder et al., 1989). The JunD expression was widespread, but not ubiquitous. There was a specific pattern of expression in different organs and cell lineages, with notable differences in differentiated cell types in organs such as kidney and testes (Fig. 3). Furthermore, in some tissues, expression was very low, e.g. in the fetal liver and the extraembryonic tissues. This is interesting in light of the tissue defects observed in c-Jun and JunB mutant embryos (Hilberg et al., 1993; Schorpp-Kistner et

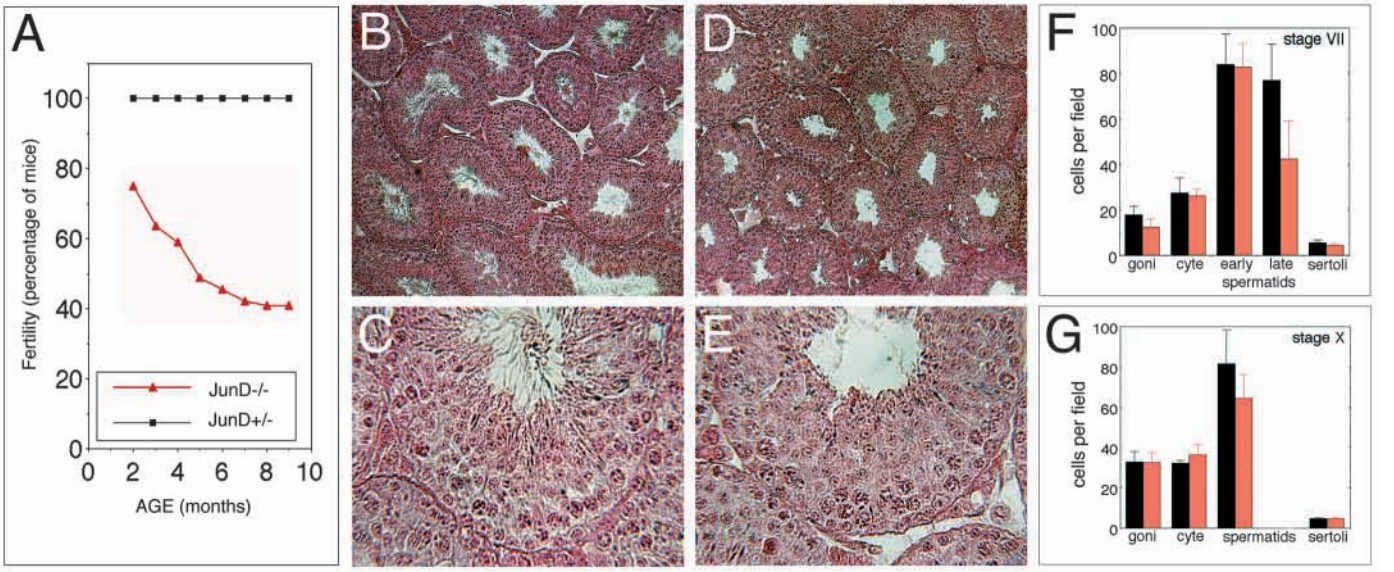

Fig. 6. Characterisation of the sterility phenotype of homozygous JunD$^{-/-}$ male mice. (A) Reduced fertility of homozygous JunD$^{-/-}$ mice. The percentage of homozygous JunD$^{-/-}$ mice capable of reproducing decreased sharply with age (triangles), while the control heterozygous animals (squares) showed no reduced fertility. (B-E) Light microscopy images of wild-type (B,C) or JunD$^{-/-}$ mutant (D,E) mouse testis histological sections stained with Hematoxylin-Eosin. At low magnification (×10 images B,D), the gross testes morphology was similar in wild-type in mutant animals. However, in mutant animals, the lumen of the tubules were often empty (D). This is clearly visible in high power (×40 magnification) images (C,E) of stage VII tubules. In JunD$^{-/-}$ mutants less late spermatids were visible and the luminal region was strikingly devoid of flagella and mature spermatozoa (E). (F,G) Quantification of different cell populations in tubules at stage VII (F) or stage X (G) of spermatogenesis. The cell numbers per high power field (×40 magnification) were determined for spermatogonia (goni), spermatocytes (cyte), early spermatids, late spermatids and Sertoli cells. Stage VII tubules showed a significant reduction in the number of late spermatids in JunD$^{-/-}$ mice (red bars), compared to fertile wild-type mice (black bars).

al., 1999). The *jun*D-*lacZ* mice will be invaluable for future detailed analysis of *jun*D expression patterns, and characterising overlapping expression patterns with other *jun* and *fos* genes.

JunD expression is dispensable for development

Despite the broad expression pattern of JunD in many cell lineages, mice lacking JunD developed normally and appeared relatively healthy, unlike mice lacking the other jun genes (Hilberg et al., 1993; Johnson et al., 1993; Schorpp-Kistner et al., 1999). Despite our observations that there is no upregulation c-*jun* and *jun*B gene expression in JunD$^{-/-}$ mice, it is possible that a functional redundancy could account for the lack of a developmental phenotype. There are several well-documented examples of genetic redundancy amongst multi-gene families of transcription factors. For example, the functional redundancy of the myoD family of myogenic regulatory factors (Rudnicki et al., 1993) or the upregulation of the bZip CREM factor explaining the mild phenotype of *CREB*$^{-/-}$ mice (Hummler et al., 1994). For the Jun family, it is possible that phenotypes are only apparent in restricted cell types where the expression patterns of the different Jun proteins do not overlap. The low levels of JunD in the liver and extraembryonic tissues may explain the hepatogenic defects of c-Jun$^{-/-}$ embryos (Hilberg et al., 1993) or placental defects in mice lacking JunB (Schorpp-Kistner et al., 1999). The recent observation that JunD interacts with menin the product of the *MEN1* tumor suppressor gene suggests that these mice will be useful in understanding menin-associated neoplasia and other JunD-related pathologies (Agarwal et al., 1999). The 30% reduction in the levels of circulating growth hormone likely contribute to the reduced postnatal growth. Furthermore, preliminary results suggest an intrinsic proliferative defects in cells lacking JunD (data not shown). Growth defects have been reported for a number of mice with disruption of genes associated with AP-1 and the cell cycle (e.g. c-*fos*$^{-/-}$ (Johnson et al., 1992), *cyclinD1*$^{-/-}$ (Sicinski et al., 1995), Rb-family members (Lee et al., 1996)).

Mutation of the *jun*D gene affects male reproductive functions

We observed specific defects in the reproductive function of JunD$^{-/-}$ male mice, indicating tissue-specific functions for JunD-containing AP-1 dimers. The sterility phenotype consists of a combination of characteristics, including both sexual behaviour and spermatogenesis. Our results suggest that the functions of JunD dimers in the pituitary and the testis are essential to maintain normal testes function. There are likely multiple factors that contribute to this complex phenotype. We have shown that changes in hormone levels and reduction in testes-specific transcription may account for some of the observed infertility. We observed a heterogeneity between homozygous JunD$^{-/-}$ males, with a clear deterioration in reproductive capacity with age. These differences could not be explained by genetic background as we observed the same phenotype even in a pure inbred 129/Sv colony. Variability of the mutation penetrance has been described in several gene targeting studies; e.g., exencephaly in a subset of p53$^{-/-}$ embryos showed (Sah et al., 1995); and variable, age-related sterility phenotypes in *BMP8* gene knockouts (Zhao et al., 1996, 1998).

Although the JunD$^{-/-}$ phenotype is unlike the embryonic lethality of other *jun* gene knockouts (Hilberg et al., 1993; Johnson et al., 1993), it resembles features observed in some *fos* gene mutations (Baum et al., 1994; Brown et al., 1996; Gruda et al., 1996; Johnson et al., 1992; Paylor et al., 1994). All published studies of *fos* family genes disruption have lead to viable mice with tissue-specific phenotypes. Disruption of the *fos*B gene caused defects in maternal nurturing behaviour (Brown et al., 1996). Mutation of the c-*fos* gene resulted in the bone remodelling disease osteopetrosis (Grigoriadis et al., 1994; Johnson et al., 1992). These c-Fos$^{-/-}$ mice also displayed variable defects in male reproduction, include reduced mating behaviour and a block in spermatogenesis (Baum et al., 1994; Johnson et al., 1992). These results are remarkably similar to our observations with JunD$^{-/-}$ mice. Male animals lacking JunD also have a reproductive defect that consists of both behavioural and spermatogenic elements, suggesting that these defects may reflect selective functions for JunD/c-Fos dimers. This is supported by the overlap of c-Fos and JunD expression patterns in postmeiotic cells (Alcivar et al., 1991; Schultz et al., 1995). Hence, JunD$^{-/-}$ mice display some features of the pleiotropic c-Fos$^{-/-}$ phenotypes and imply tissue-specific roles for JunD/c-Fos dimers in maintaining normal spermatogenesis and reproductive functions.

The block in spermatogenesis upon JunD disruption appears not to be a cell autonomous defect, as haploid sperm are transmitted to offspring at equivalent frequencies as wild-type sperm. Crosses between heterozygous JunD$^{+/-}$ males and wild-type females generated both JunD$^{+/-}$ and wild-type offspring with equal numbers (e.g. 53 heterozygotes: 52 wild-type) and crosses between heterozygous animals generated all three genotypes at predicted frequencies.

JunD can now be added to a growing number of genes that affect male fertility (Elliott and Cooke, 1997). Ordering these

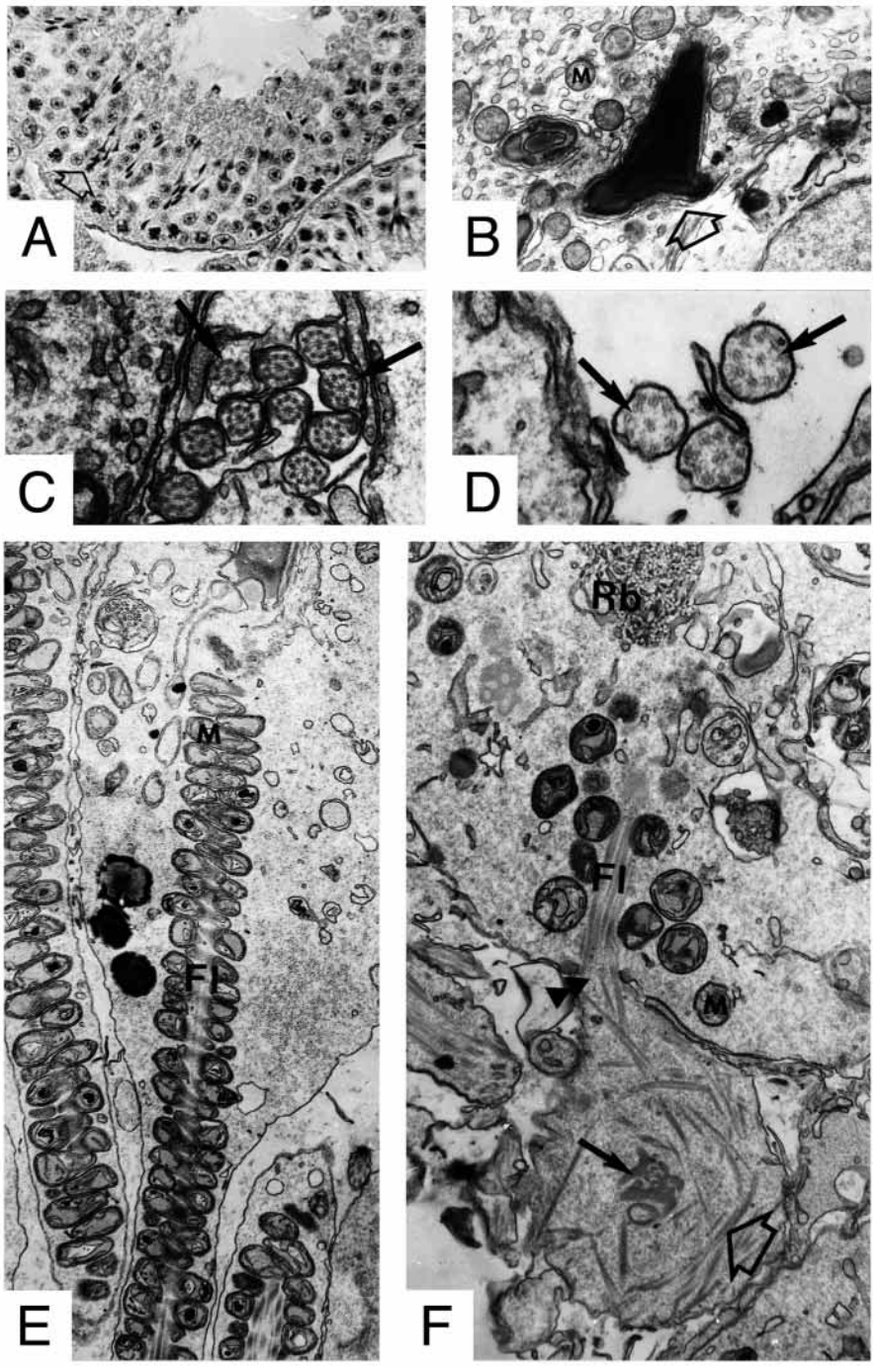

Fig. 7. Characterisation of spermatozoa defects in sterile JunD$^{-/-}$ mice. (A,B) Defects in head structures. (A) Light microscopy of a Stage V seminiferous tubule of an homozygous JunD$^{-/-}$ mutant. The late spermatids present between the other germ cells show abnormal hammer-like head shape (open arrow). (B) Electronic microscopy image of the same animal; the misshapen head of late spermatids is dramatic (open arrow). Mitochondria of the surrounding Sertoli cells are visible (M). (C-F) Defects in flagella structures. Ultrastructural examination of the germ cell defects of JunD$^{-/-}$ sterile mice. (C) Images of a tubule from a wild-type animal showing a cross section through several flagella (arrows indicate their regular nine microtubule doublets), which are tightly clustered between germ cells. (D) Cross section of tubules at the same stage in a hypo-fertile JunD$^{-/-}$ mutant mice – sections containing flagella are very rare and when seen they appear abnormal and not well organised (E). Longitudinal section of a late spermatid (stage V-VI) in a wild-type animal. The mitochondrial (M) sheath surrounds the elongated flagellum (Fl). (F) Longitudinal section of a late spermatid (stage V-VI) in a homozygous JunD$^{-/-}$ mutant animal. Although the mitochondria are visible (M), there is a clear disorganisation of the flagella as it elongates from the spermatid (double arrowhead). The periaxonemal cytoplasm bulged out, forming irregular cytoplasmic masses (open arrowhead). This irregularly shaped periaxonemal cytoplasm still contained clusters of electron-dense material, as well as disorganised small microtubules (small arrow).

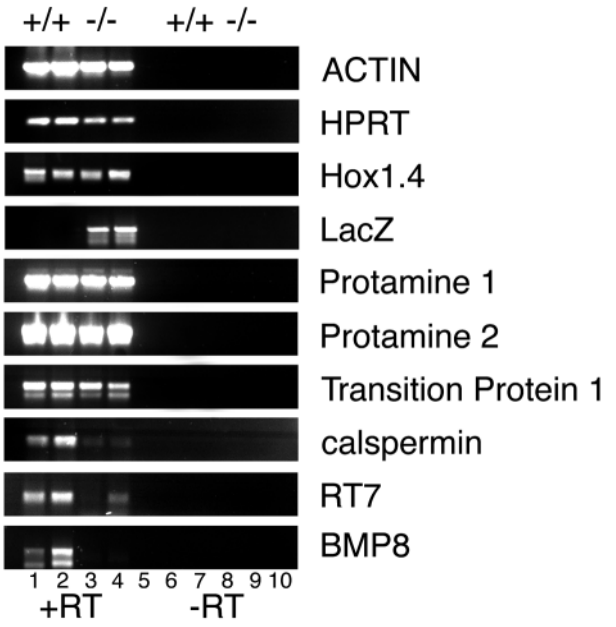

Fig. 8. Analysis of gene expression in testes of sterile JunD$^{-/-}$ mice. The expression of genes involved in spermatogenesis was determined using an RT-PCR assay. Total RNA was isolated from the testes of two wild-type animals (+/+) and two sterile mutant animals (–/–). The expression levels of several genes were examined by PCR following treatment with reverse transcriptase (lanes 1-5, +RT). The expression of β-actin and HPRT were included as positive controls. Amplification of samples not treated with reverse transcriptase (lanes 6-10, –RT) or water alone (lanes 5 and 10) served as negative controls. The expression analysis includes the bacterial *lacZ* gene used for insertional mutagenesis, and spermatogenesis-related genes protamine 1, protamine 2, Transition protein 1, *Hox1.4*, *calspermin*, *RT7* and *BMP8*.

genes on regulatory pathways during spermatogenesis presents a formidable goal for future studies. Genes whose mutation affects mouse fertility can be divided into several classes of phenotypes. These include phenotypes that are predominantly behavioural (e.g. SP4 (Supp et al., 1996)), those affecting spermatozoa fertilisation capacity (e.g. genes for sperm-1 or angiotensin converting enzyme (ACE) (Hagaman et al., 1998; Pearse et al., 1997)) and those affecting specific spermatogenic cell types (e.g. RXRβ (Kastner et al., 1996)). Perhaps the most interesting genes with respect to our study are *CREM* and *BMP8*. Mutation of the murine *CREM* gene lead to a similar block in spermiogenesis with the lack of late spermatids and mature spermatozoa (Blendy et al., 1996; Nantel et al., 1996). CREM is a related bZip factor and can bind to CRE sites which are present in the promoters of several spermatogenesis-related genes. In the testes of CREM$^{-/-}$ mice, there is a loss of expression of a number of spermatogenesis-related genes. Our analysis shows that only a subset of these genes is lost in JunD$^{-/-}$ mice (Fig. 8), suggesting overlapping functions for the JunD and CREM factors. BMP8 belongs to the mammalian TGFβ superfamily. Murine *BMP8* genes are essential for germ cell proliferation and maintaining adult spermatogenesis (Zhao et al., 1996, 1998). This is of interest in light of the recent observations that the *Drosophila* TGFβ homologue *dpp*, is a potential downstream target of *Drosophila* Jun (Martin-Blanco, 1997) and is important for the maintenance of female germline stem cells (Ting and Spradling, 1998).

Human infertility may affect as much as 2-7 % of the population and is often ascribed to idiopathic abnormalities in sperm numbers (azoospermia or oligospermia) and sperm motility. Very few genes associated with human azoospermia have been identified (Reijo et al., 1995) and the genetic basis for human male sterility remains unclear (Elliott and Cooke, 1997). Several features of the JunD sterility phenotype resemble aspects of human reproductive pathology suggesting that these animals may contribute to our understanding and treatment of human infertility.

We thank C. Kress for the CK35 ES cells, P. Brulet and L. Coen for the 129/Sv mouse genomic library, L. Fiette and P. Ave for histological analysis, L. Lepourry for help with animal care, and E. Bois for genotype analysis. We are grateful to members of the Yaniv laboratory for helpful discussions and advice. This work was supported by funding from the ARC, the LNFCC, the EC Biomed and Training and Mobility Programs and by a TMR Postdoctoral Fellowship to J. B. W.

REFERENCES

Agarwal, S. K., Guru, S. C., Heppner, C., Erdos, M. R., Collins, R. M., Park, S. Y., Saggar, S., Chandrasekharappa, S. C., Collins, F. S., Spiegel, A. M. et al. (1999). Menin interacts with the AP1 transcription factor JunD and represses JunD-activated transcription. *Cell* **96**, 143-152.

Albert, M. and Roussel, C. (1984). Strain differences in the concentration, motility and morphology of epididymal sperm in relation to puberty in mice. *Int J Androl* **7**, 334-347.

Alcivar, A. A., Hake, L. E., Kwon, Y. K. and Hecht, N. B. (1991). junD mRNA expression differs from c-jun and junB mRNA expression during male germinal cell differentiation. *Mol. Reprod. Dev.* **30**, 187-193.

Angel, P., Allegretto, E. A., Okino, S. T., Hattori, K., Boyle, W. J., Hunter, T. and Karin, M. (1988). Oncogene jun encodes a sequence-specific trans-activator similar to AP- 1. *Nature* **332**, 166-171.

Angel, P. and Karin, M. (1991). The role of Jun, Fos and the AP-1 complex in cell-proliferation and transformation. *Biochim. Biophys. Acta* **1072**, 129-157.

Baum, M. J., Brown, J. J., Kica, E., Rubin, B. S., Johnson, R. S. and Papaioannou, V. E. (1994). Effect of a null mutation of the c-fos proto-oncogene on sexual behavior of male mice. *Biol. Reprod.* **50**, 1040-1048.

Blendy, J. A., Kaestner, K. H., Weinbauer, G. F., Nieschlag, E. and Schutz, G. (1996). Severe impairment of spermatogenesis in mice lacking the CREM gene. *Nature* **380**, 162-165.

Bohmann, D., Bos, T. J., Admon, A., Nishimura, T., Vogt, P. K. and Tjian, R. (1987). Human proto-oncogene c-jun encodes a DNA binding protein with structural and functional properties of transcription factor AP-1. *Science* **238**, 1386-1392.

Bossy-Wetzel, E., Bakiri, L. and Yaniv, M. (1997). Induction of apoptosis by the transcription factor c-Jun. *EMBO J.* **16**, 1695-1709.

Bradley, A. (1987). Production and analysis of chimeric mice. In *Teratocarcinomas and Embryonic Stem cells; a Practical Approach*. (ed. E. J. Robertson). pp. 113-151. Oxford: IRL Press.

Brown, J. R., Ye, H., Bronson, R. T., Dikkes, P. and Greenberg, M. E. (1996). A defect in nurturing in mice lacking the immediate early gene fosB. *Cell* **86**, 297-309.

Camus, A., Kress, C., Babinet, C. and Barra, J. (1996). Unexpected behavior of a gene trap vector comprising a fusion between the Sh ble and the lacZ genes. *Mol. Reprod. Dev.* **45**, 255-263.

Chiu, R., Angel, P. and Karin, M. (1989). Jun-B differs in its biological properties from, and is a negative regulator of, c-Jun. *Cell* **59**, 979-986.

Cohen, D. R., Vandermark, S. E., McGovern, J. D. and Bradley, M. P. (1993). Transcriptional regulation in the testis: a role for transcription factor AP-1 complexes at various stages of spermatogenesis. *Oncogene* **8**, 443-455.

Colucci-Guyon, E., Portier, M. M., Dunia, I., Paulin, D., Pournin, S. and

Babinet, C. (1994). Mice lacking vimentin develop and reproduce without an obvious phenotype. *Cell* **79**, 679-694

Elliott, D. J. and Cooke, H. J. (1997). The molecular genetics of male infertility. *BioEssays* **19**, 801-809.

Grigoriadis, A. E., Wang, Z. Q., Cecchini, M. G., Hofstetter, W., Felix, R., Fleisch, H. A. and Wagner, E. F. (1994). c-Fos: a key regulator of osteoclast-macrophage lineage determination and bone remodeling. *Science* **266**, 443-448.

Gruda, M. C., van Amsterdam, J., Rizzo, C. A., Durham, S. K., Lira, S. and Bravo, R. (1996). Expression of FosB during mouse development: normal development of FosB knockout mice. *Oncogene* **12**, 2177-2185.

Hagaman, J. R., Moyer, J. S., Bachman, E. S., Sibony, M., Magyar, P. L., Welch, J. E., Smithies, O., Krege, J. H. and O'Brien, D. A. (1998). Angiotensin-converting enzyme and male fertility. *Proc. Natl. Acad. Sci. USA* **95**, 2552-2557.

Hai, T. W., Liu, F., Coukos, W. J. and Green, M. R. (1989). Transcription factor ATF cDNA clones: an extensive family of leucine zipper proteins able to selectively form DNA-binding heterodimers. *Genes Dev.* **3**, 2083-2090.

Ham, J., Babij, C., Whitfield, J., Pfarr, C. M., Lallemand, D., Yaniv, M. and Rubin, L. L. (1995). A c-Jun dominant negative mutant protects sympathetic neurons against programmed cell death. *Neuron* **14**, 927-939.

Hilberg, F., Aguzzi, A., Howells, N. and Wagner, E. F. (1993). c-jun is essential for normal mouse development and hepatogenesis. *Nature* **365**, 179-181.

Hirai, S. I., Ryseck, R. P., Mechta, F., Bravo, R. and Yaniv, M. (1989). Characterization of junD: a new member of the jun proto-oncogene family. *EMBO J.* **8**, 1433-1439.

Hummler, E., Cole, T. J., Blendy, J. A., Ganss, R., Aguzzi, A., Schmid, W., Beermann, F. and Schutz, G. (1994). Targeted mutation of the CREB gene: compensation within the CREB/ATF family of transcription factors. *Proc. Natl Acad. Sci. USA* **91**, 5647-5651.

Johnson, R., Spiegelman, B., Hanahan, D. and Wisdom, R. (1996). Cellular transformation and malignancy induced by ras require c-jun. *Mol. Cell Biol.* **16**, 4504-4511

Johnson, R. S., Spiegelman, B. M. and Papaioannou, V. (1992). Pleiotropic effects of a null mutation in the c-fos proto-oncogene. *Cell* **71**, 577-586.

Johnson, R. S., van Lingen, B., Papaioannou, V. E. and Spiegelman, B. M. (1993). A null mutation at the c-jun locus causes embryonic lethality and retarded cell growth in culture. *Genes Dev*. **7**, 1309-1317.

Kallunki, T., Deng, T., Hibi, M. and Karin, M. (1996). c-Jun can recruit JNK to phosphorylate dimerization partners via specific docking interactions. *Cell* **87**, 929-939.

Karnovsky, M. (1971). Use of ferrocyanide-reduced osmium tetroxide in electron microscopy. *J. Cell Biol.* **51**, 284.

Kastner, P., Mark, M., Leid, M., Gansmuller, A., Chin, W., Grondona, J. M., Decimo, D., Krezel, W., Dierich, A. and Chambon, P. (1996). Abnormal spermatogenesis in RXRβ mutant mice. *Genes Dev.* **10**, 80-92.

Kouzarides, T. and Ziff, E. (1988). The role of the leucine zipper in the fos-jun interaction. *Nature* **336**, 646-651.

Kovary, K. and Bravo, R. (1991). Expression of different Jun and Fos proteins during the G0-to-G1 transition in mouse fibroblasts: in vitro and in vivo associations. *Mol. Cell Biol.* **11**, 2451-2459.

Kress, C., Vandormael, P. S., Baldacci, P., Cohen, T. M. and Babinet, C. (1998). Nonpermissiveness for mouse embryonic stem (ES) cell derivation circumvented by a single backcross to 129/Sv strain: establishment of ES cell lines bearing the omd conditional lethal mutation. *Mamm. Genome* **9**, 998-1001

Lallemand, D., Spyrou, G., Yaniv, M. and Pfarr, C. M. (1997). Variations in Jun and Fos protein expression and AP-1 activity in cycling, resting and stimulated fibroblasts. *Oncogene* **14**, 819-830.

Landschulz, W. H., Johnson, P. F. and McKnight, S. L. (1988). The leucine zipper: a hypothetical structure common to a new class of DNA binding proteins. *Science* **240**, 1759-1764.

Lee, M. H., Williams, B. O., Mulligan, G., Mukai, S., Bronson, R. T., Dyson, N., Harlow, E. and Jacks, T. (1996). Targeted disruption of p107: functional overlap between p107 and Rb. *Genes Dev.* **10**, 1621-1632.

Mansour, S. L., Goddard, J. M. and Capecchi, M. R. (1993). Mice homozygous for a targeted disruption of the proto-oncogene int-2 have developmental defects in the tail and inner ear. *Development* **117**, 13-28.

Martin-Blanco, E. (1997). Regulation of cell differentiation by the Drosophila Jun kinase cascade. *Curr. Opin. Genet. Dev.* **7**, 666-671.

Mechta, F., Lallemand, D., Pfarr, C. M. and Yaniv, M. (1997). Transformation by ras modifies AP1 composition and activity. *Oncogene* **14**, 837-847.

Nakabeppu, Y., Ryder, K. and Nathans, D. (1988). DNA binding activities of three murine Jun proteins: stimulation by Fos. *Cell* **55**, 907-915.

Nantel, F., Monaco, L., Foulkes, N. S., Masquilier, D., LeMeur, M., Henriksen, K., Dierich, A., Parvinen, M. and Sassone-Corsi, P. (1996). Spermiogenesis deficiency and germ-cell apoptosis in CREM-mutant mice. *Nature* **380**, 159-162.

Paylor, R., Johnson, R. S., Papaioannou, V., Spiegelman, B. M. and Wehner, J. M. (1994). Behavioral assessment of c-fos mutant mice. *Brain Res.* **651**, 275-282.

Pearse, R. n., Drolet, D. W., Kalla, K. A., Hooshmand, F., Bermingham, J. J. and Rosenfeld, M. G. (1997). Reduced fertility in mice deficient for the POU protein sperm-1. *Proc. Natl Acad. Sci. USA* **94**, 7555-7560.

Pfarr, C. M., Mechta, F., Spyrou, G., Lallemand, D., Carillo, S. and Yaniv, M. (1994). Mouse JunD negatively regulates fibroblast growth and antagonizes transformation by ras. *Cell* **76**, 747-760.

Reijo, R., Lee, T. Y., Salo, P., Alagappan, R., Brown, L. G., Rosenberg, M., Rozen, S., Jaffe, T., Straus, D., Hovatta, O. et al. (1995). Diverse spermatogenic defects in humans caused by Y chromosome deletions encompassing a novel RNA-binding protein gene. *Nat. Genet.* **10**, 383-393.

Reimold, A. M., Grusby, M. J., Kosaras, B., Fries, J. W., Mori, R., Maniwa, S., Clauss, I. M., Collins, T., Sidman, R. L., Glimcher, M. J. et al. (1996). Chondrodysplasia and neurological abnormalities in ATF-2-deficient mice. *Nature* **379**, 262-265.

Rudnicki, M. A., Schnegelsberg, P. N., Stead, R. H., Braun, T., Arnold, H. H. and Jaenisch, R. (1993). MyoD or Myf-5 is required for the formation of skeletal muscle. *Cell* **75**, 1351-1359.

Rutberg, S. E., Saez, E., Glick, A., Dlugosz, A. A., Spiegelman, B. M. and Yuspa, S. H. (1996). Differentiation of mouse keratinocytes is accompanied by PKC-dependent changes in AP-1 proteins. *Oncogene* **13**, 167-176.

Ryder, K., Lanahan, A., Perez, A. E. and Nathans, D. (1989). jun-D: a third member of the jun gene family. *Proc. Natl Acad. Sci. USA* **86**, 1500-1503.

Ryseck, R. P., Hirai, S. I., Yaniv, M. and Bravo, R. (1988). Transcriptional activation of c-jun during the G0/G1 transition in mouse fibroblasts. *Nature* **334**, 535-537.

Sah, V. P., Attardi, L. D., Mulligan, G. J., Williams, B. O., Bronson, R. T. and Jacks, T. (1995). A subset of p53-deficient embryos exhibit exencephaly. *Nat. Genet.* **10**, 175-180.

Sassone-Corsi, P., Ransone, L. J., Lamph, W. W. and Verma, I. M. (1988). Direct interaction between fos and jun nuclear oncoproteins: role of the 'leucine zipper' domain. *Nature* **336**, 692-695.

Schorpp-Kistner, M., Wang, Z.-Q., Angel, P. and Wagner, E. F. (1999). JunB is essential for mammalian placentation. *EMBO J.* **18**, 934-948.

Schultz, R., Penttila, T. L., Parvinen, M., Persson, H., Hokfelt, T. and Pelto-Huikko, M. (1995). Expression of immediate early genes in tubular cells of rat testis. *Biol. Reprod.* **52**, 1215-1226.

Sicinski, P., Donaher, J. L., Parker, S. B., Li, T., Fazeli, A., Gardner, H., Haslam, S. Z., Bronson, R. T., Elledge, S. J. and Weinberg, R. A. (1995). Cyclin D1 provides a link between development and oncogenesis in the retina and breast. *Cell* **82**, 621-630.

Smeal, T., Binetruy, B., Mercola, D. A., Birrer, M. and Karin, M. (1991). Oncogenic and transcriptional cooperation with Ha-Ras requires phosphorylation of c-Jun on serines 63 and 73. *Nature* **354**, 494-496.

Supp, D. M., Witte, D. P., Branford, W. W., Smith, E. P. and Potter, S. S. (1996). Sp4, a member of the Sp1-family of zinc finger transcription factors, is required for normal murine growth, viability, and male fertility. *Dev. Biol.* **176**, 284-299.

Ting, X. and Spradling, A. (1998). decapentaplegic is essential for the maintenance and division of germline stem cells in the Drosophila ovary. *Cell* **94**, 251-260.

Wang, Z. Q., Ovitt, C., Grigoriadis, A. E., Mohle, S. U., Ruther, U. and Wagner, E. F. (1992). Bone and haematopoietic defects in mice lacking c-fos. *Nature* **360**, 741-745.

Wilkinson, D. G., Bhatt, S., Ryseck, R. P. and Bravo, R. (1989). Tissue-specific expression of c-jun and junB during organogenesis in the mouse. *Development* **106**, 465-471.

Zhao, G. Q., Deng, K., Labosky, P. A., Liaw, L. and Hogan, B. L. (1996). The gene encoding bone morphogenetic protein 8B is required for the initiation and maintenance of spermatogenesis in the mouse. *Genes Dev.* **10**, 1657-1669.

Zhao, G. Q., Liaw, L. and Hogan, B. L. (1998). Bone morphogenetic protein 8A plays a role in the maintenance of spermatogenesis and the integrity of the epididymis. *Development* **125**, 1103-1112.